



Article

# Manganese and Cobalt Doped Hierarchical Mesoporous Halloysite-Based Catalysts for Selective Oxidation of *p*-Xylene to Terephthalic Acid

Eduard Karakhanov<sup>1</sup>, Anton Maximov<sup>1,2</sup>, Anna Zolotukhina<sup>1,2</sup>, Vladimir Vinokurov<sup>3</sup>,  
Evgenii Ivanov<sup>3</sup>  and Aleksandr Glotov<sup>3,\*</sup> 

<sup>1</sup> Department of Petroleum Chemistry and Organic Catalysis, Moscow State University, 119991 Moscow, Russia; kar@petrol.chem.msu.ru (E.K.); max@ips.ac.ru (A.M.); anisole@yandex.ru (A.Z.)

<sup>2</sup> A.V. Topchiev Institute of Petrochemical Synthesis, Russian Academy of Sciences, 119991 Moscow, Russia

<sup>3</sup> Department of Physical and Colloid Chemistry, Gubkin Russian State University of Oil and Gas, 119991 Moscow, Russia; vinok\_ac@mail.ru (V.V.); ivanov166@list.ru (E.I.)

\* Correspondence: glotov.a@gubkin.ru

Received: 18 November 2019; Accepted: 14 December 2019; Published: 18 December 2019



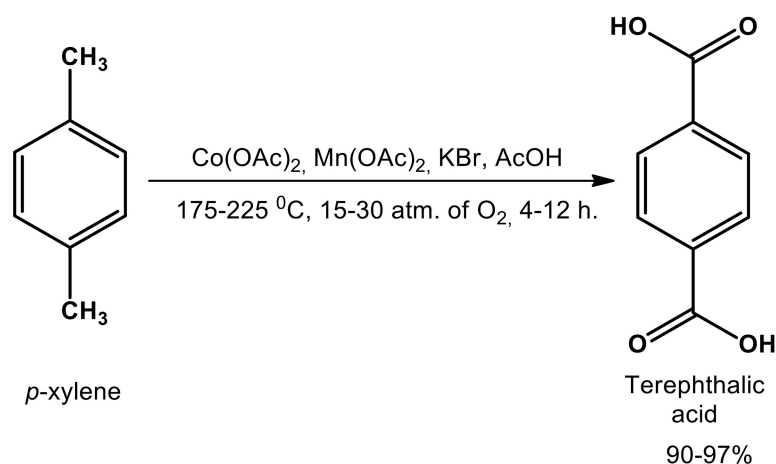
**Abstract:** Bimetallic MnCo catalyst, supported on the mesoporous hierarchical MCM-41/halloysite nanotube composite, was synthesized for the first time and proved its efficacy in the selective oxidation of *p*-xylene to terephthalic acid under conditions of the AMOCO process. Quantitative yields of terephthalic acid were achieved within 3 h at 200–250 °C, 20 atm. of O<sub>2</sub> and at a substrate to the Mn + Co ratio of 4–4.5 times higher than for traditional homogeneous system. The influence of temperature, oxygen, pressure and KBr addition on the catalyst activity was investigated, and the mechanism for the oxidation of *p*-toluic acid to terephthalic acid, excluding undesirable 4-carboxybenzaldehyde, was proposed.

**Keywords:** halloysite; hierarchical materials; *p*-xylene oxidation; terephthalic acid

## 1. Introduction

Terephthalic acid (TPA) and its dimethyl ester are important monomers in thermoresistant and mechanically stable polymer production, such as polyethylene terephthalate (PET) and poly-paraphenylene terephthalamide (Kevlar) [1,2]. The world production of terephthalic acid has exceeded 5 Mt/yr. is still growing [1,2]. Currently up to 70% of terephthalic acid is produced by direct oxidation of *p*-xylene through the AMOCO/Mid-Century process being developed in the 1960s [1–6].

*p*-xylene in the AMOCO process is subjected to oxidation by molecular oxygen or air in the presence of homogeneous Mn and Co catalysts with KBr as a promotor and free-radical source in acetic acid medium under the severe conditions (170–220 °C, 15–30 atm of O<sub>2</sub> or 50–70 atm of air), giving terephthalic acid yield of 90–97% within 4–12 h (Scheme 1) [7–10].



**Scheme 1.** Oxidation of *p*-xylene to terephthalic acid in the AMOCO process [1,2,7,8].

In spite of the obvious advantage of the AMOCO process, such as quantitative yield of high purity terephthalic acid, acetic acid medium with bromides cause corrosion that makes it necessary to use expensive titanium reactors [11–13]. It challenges the development of new environmentally friendly, safer and less corrosive reaction media, promoters and additives [7]. Catalyst heterogenization is considered as one of the possible ways for improving the AMOCO process.

Thus, it was earlier demonstrated, that the use of CoO and Co<sub>3</sub>O<sub>4</sub> as catalysts together in the presence of MnO, NiO or CeO co-catalysts and *p*-toluic acid as a promotor allowed for oxidation without KBr [14]. Nonetheless, this system appeared to be much less effective in comparison with the conventional homogeneous system, including Mn(OAc)<sub>2</sub>, Co(OAc)<sub>2</sub> and KBr, and the yield of terephthalic acid did not exceed 65–70% within 8 h [14].

In the presence of MCM-41 doped with Fe and Cu, terephthalic acid underwent further oxidation to 2,5-dihydroxy-1,4-terephthalic and *p*-benzoquinone-2,5-dicarboxylic acids even under much milder conditions, than in the AMOCO process (H<sub>2</sub>O<sub>2</sub> as an oxidant, 80 °C, AcOH, CH<sub>3</sub>CN, 5 h) [15]. The highest selectivity to terephthalic acid did not exceed 45% at a *p*-xylene conversion of 10% in the neat acetonitrile. It was found out, that iron additive increased the selectivity to terephthalic acid, whereas copper addition, vice versa, favored the further oxidation of TPA to 2,5-dihydroxy-1,4-terephthalic and *p*-benzoquinone-2,5-dicarboxylic acids [15].

High yields of terephthalic acid (99% within 2 h) were obtained in the presence of polynuclear μ<sub>3</sub>-oxo-bound complexes of Co and Mn, encapsulated in the cavities of Y zeolite, under the conditions similar to AMOCO process (KBr, 200 °C, 610 atm of the air) [16]. The said catalyst appeared as highly resistant to the metal leaching due to close sizes of polyoxo metal clusters and zeolite cavities [8,16].

In this connection, halloysite-based materials appeared to be promising as heterogeneous catalysts for *p*-xylene oxidation under the typical conditions. Halloysite is a natural clay with the rolled tubular structure, appearing as a multiwall nanotube (halloysite nanotube, HNT) with a length of 0.5–1.5 μm, an outer diameter of 50–60 nm and an inner cavity diameter of 10–15 nm (Figure 1) [17,18]. Halloysite clays were successfully applied as carriers for the tubular Ru nanocatalysts, revealing high activity in the hydrogenations of aromatic compounds and phenols [19–23].

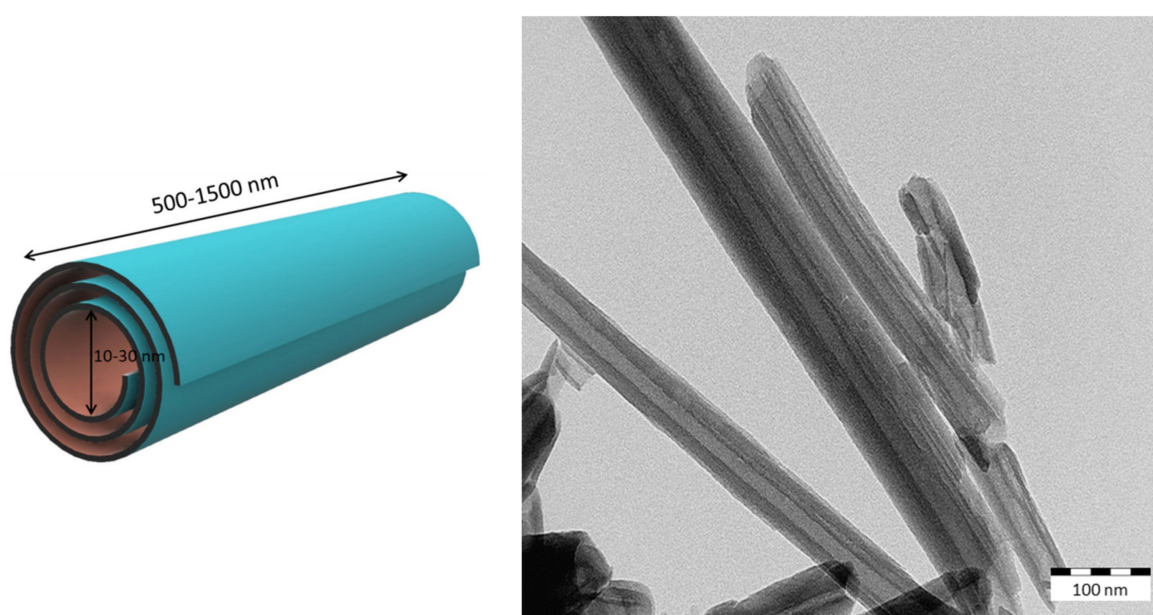


**Figure 1.** Schematic visualization (left) and TEM image (right) of halloysite clay.

Grafting of the ordered mesoporous materials, such as MCM-41 or SBA-15, onto halloysite template allows us to obtain new hierarchical systems with stronger mechanical properties and surface area up to  $650 \text{ m}^2/\text{g}$  (Figure 2) [21,24,25]. La-doped MCM-41/HNT composite revealed high efficacy as a sulfur-reducing additive for FCC (fluid catalytic cracking) catalyst, resulting in decrease of sulfur content by 25% and in the yield of gasoline fraction of about 45% [24,26,27]. Modified with CaO and MgO, MCM-41/HNT and SBA-15/HNT composites demonstrated high activity in the cracking of sulfones, formed after the oxidative desulfurization of diesel fraction, decreasing sulfur content from 450 up to 100 ppm [28]. The catalysts said were recycled several times without significant loss of activity, and with high resistance to metal leaching and structure maintenance under the reaction conditions [28].

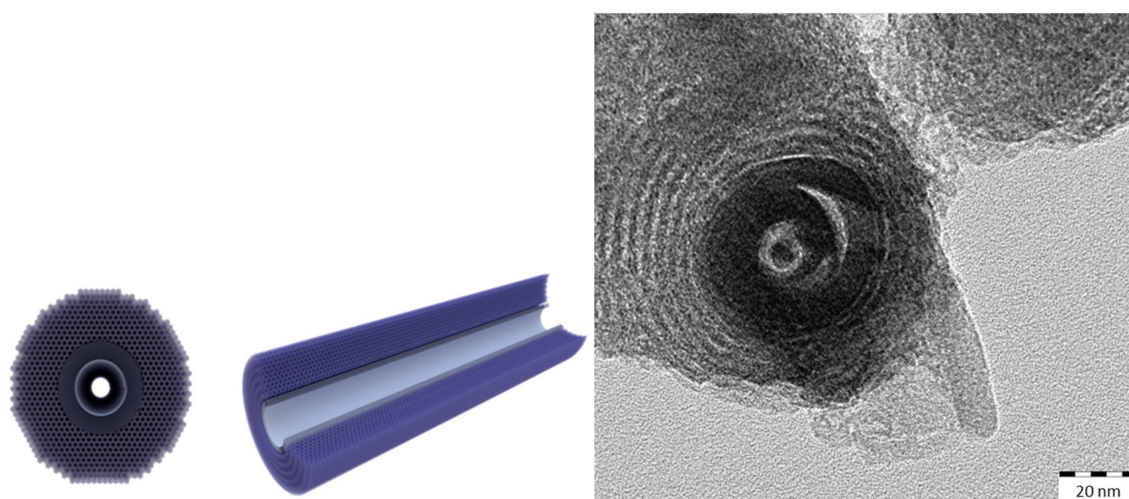


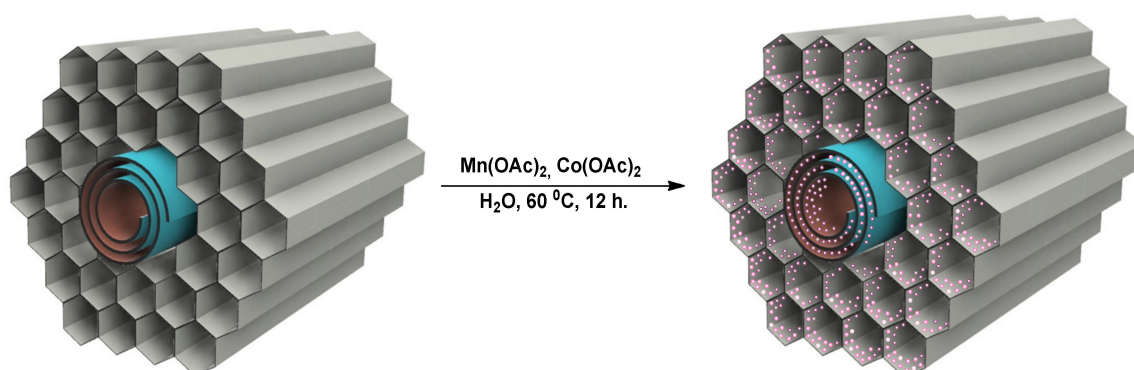
**Figure 2.** Schematic visualization (left) and TEM image (right) of MCM-41/HNT composite.

In this work, we present for the first-time synthesis of new heterogeneous bimetallic MnCo catalyst, based on mesoporous hierarchical MCM-41/HNT composite that can be successfully applied for quantitative oxidation of *p*-xylene to terephthalic acid in the AMOCO process, proving its efficiency, that was 4–4.5 times higher, as compared with a traditional homogeneous system.

## 2. Results and Discussion

### 2.1. The Synthesis and Characterization of Hierarchical Mesoporous MCM-41/HNT Composite, Doped with Mn and Co

Bimetallic MnCo catalyst, based on MCM-41/HNT composite was synthesized by the wetness impregnation method. Herein  $Mn^{2+}$  and  $Co^{2+}$  were deposited from the water solution of  $Mn(OAc)_2$  and  $Co(OAc)_2$  in molar ratio of 1:10 (Scheme 2) [16].  $Mn(OAc)_2$  and  $Co(OAc)_2$  tetrahydrates were chosen as sources for  $Mn^{2+}$  and  $Co^{2+}$  respectively to avoid the influence of other counter-anions on the adsorption and oxidation processes, and because of acetic acid, used as a solvent in the conventional oxidation process [2,8].



**Scheme 2.**  $Mn(OAc)_2$  and  $Co(OAc)_2$  deposition onto MCM-41/HNT composite.

The material obtained was characterized by atomic emission spectroscopy with inductively coupled plasma (ICP-AES), transmission electron microscopy (TEM) and X-ray photoelectron spectroscopy (XPS). The physical and chemical properties are listed in Table 1.

**Table 1.** Physical and chemical properties of the synthesized  $Mn^{II}_1Co^{II}_{10}@MCM-41/HNT$  catalyst.

Mn (wt. %)	Co (wt. %)	Surface Concentration by XPS, at. %							Mn Valency States at Mn 2p <sub>3/2</sub> Line, at. %		Co Valency States at Co 2p <sub>3/2</sub> Line, at. %	
		Mn	Co	Si	Al	C	N	O	MnO (eV)	[MnO <sub>4</sub> ] Bound (eV)	CoO (eV)	[CoO <sub>6</sub> ] Bound (eV)
0.15	1.29	<0.1	0.7	25.9	2.5	5.8	0.6	64.2	79.8 (642.5)	20.2 (646.9)	15.3 (780.0)	84.7 (782.5)

As seen from Table 1, weight content of Mn and Co in the sample reached 0.15% and 1.29% respectively, which was approximately three times less than corresponding theoretical values. Herein Co/Mn ratio appeared as 8.6:1, which was in accordance with the literature data [29].

According to XPS data (Table 1, Figure 3), both Mn and Co were presented in the forms of simple oxides MnO [30–32] and CoO [33–35] and bound complexes [MnO<sub>4</sub>] [36,37] and [CoO<sub>6</sub>] [32–34,38–41], arising from initial  $Mn(OAc)_2$  and  $Co(OAc)_2$  tetrahydrates as well as from the aluminosilicate. Herein MnO form strongly predominated over [MnO<sub>4</sub>] bound form for Mn, whereas for Co [CoO<sub>6</sub>] form, vice versa, predominated over CoO, that might be due to the much stronger oxygen affinity for Co in comparison with Mn [42,43]. Taking in account the presence of nitrogen in the XPS spectra (Table 1), carbon in the sample, found out in  $-CH_2CH_2-$ ,  $-CH_2CH_2N-$  and  $H_3CC(=O)-$  forms [44,45], may be related not only to adsorbed acetate anions, but also to cetyl trimethyl ammonium bromide template, partly remained in the MCM-41/HNT composite after calcination.



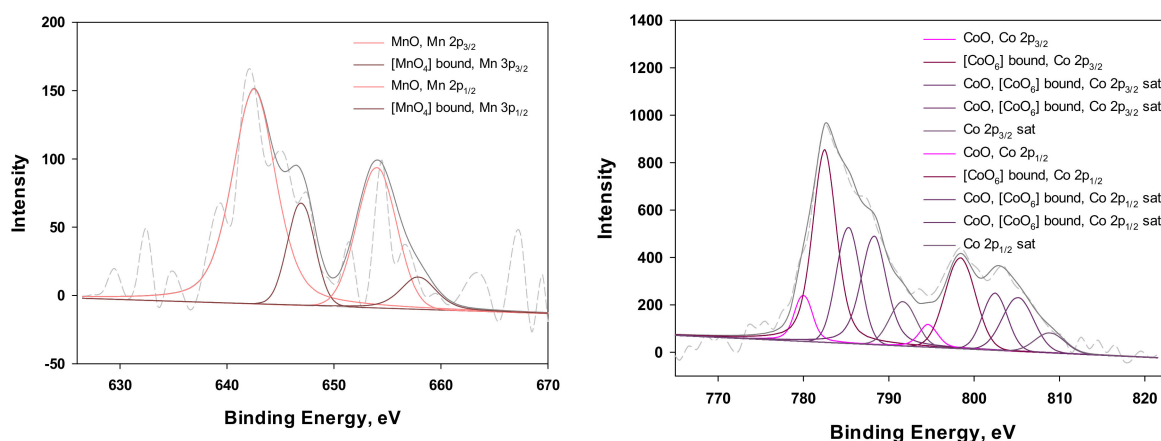


**Figure 3.** XPS spectra of Mn (left) and Co (right) in  $\text{Mn}^{\text{II}}_1\text{Co}^{\text{II}}_{10}\text{@MCM-41/HNT}$  composite at 2p line.

As TEM analysis showed (Figure 4), deposition of manganese and cobalt acetates did not destruct the MCM-41/HNT matrix. The MCM-41 framework observed consisted of regular hexagonal pores of 2.9 nm in diameter (Figure 4B) and inner located halloysite nanotubes with the inner diameter of 12–15 nm and outer diameter of 31–35 nm, and interplanar space of 3.2 nm (Figure 4A).

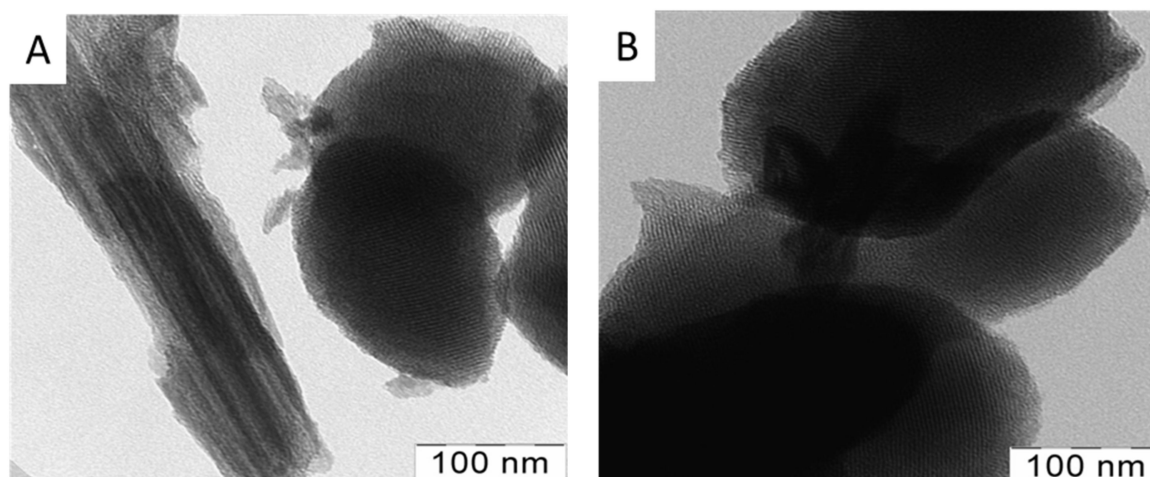
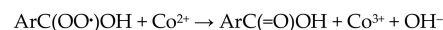
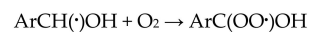
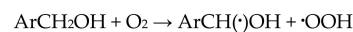
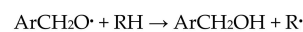
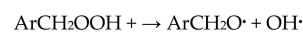
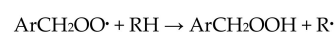
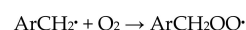
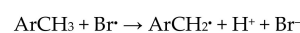
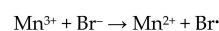
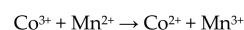
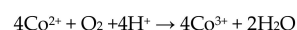
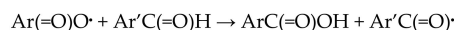
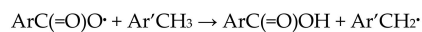
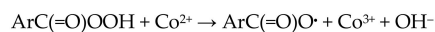
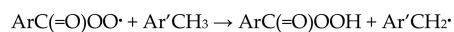
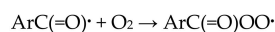
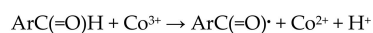
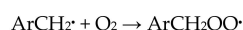
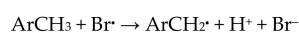
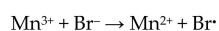
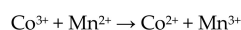
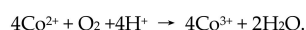
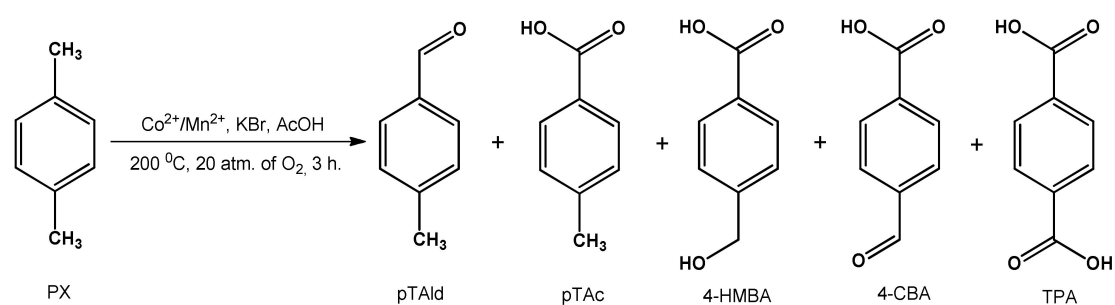


**Figure 4.** TEM images of MCM-41/HNT composite (A—HNT templated MCM-41, B—MCM-41) after deposition of  $\text{Mn}(\text{OAc})_2$  and  $\text{Co}(\text{OAc})_2$ .

## 2.2. Oxidation of *p*-Xylene in the Presence of Hierarchical Mesoporous MCM-41/HNT Composite Doped with Mn and Co

The catalyst synthesized was tested in the liquid-phase oxidation of *p*-xylene and compared with traditional homogeneous system  $\text{Mn}(\text{OAc})_2/\text{Co}(\text{OAc})_2/\text{KBr}$ . It should be noted, that *p*-xylene oxidation is a multi-stage radical process (Scheme 3) [2,7,8,46,47]. Its kinetics is strongly affected by the reaction conditions, such as temperature, oxygen pressure, substrate concentration, substrate: Co:Mn ratios, KBr loading, etc. [2,7,8]. Herein KBr is required as a free radical source, and  $\text{Mn}(\text{OAc})_2$  acts as promotor at the first stage of reaction—activation of the methyl group in the *p*-xylene molecule [2,10]. As a rule, *p*-xylene conversion to *p*-toluic acid proceeds fast, whereas oxidation thereof to terephthalic acid is a slow highly activated process [2,8]. The use of acetic acid as a solvent promotes dissolution of both KBr and *p*-xylene, the ion-radical oxidation process, and deposition of terephthalic acid due to its poor solubility. The TPA product is easily isolated from the reaction medium as white needle-like glittering crystals [2].



**Scheme 3.** Radical involved mechanism of *p*-xylene oxidation in the presence of  $\text{Mn}^{2+}/\text{Co}^{2+}/\text{KBr}/\text{AcOH}$  system [2,7,8].

The best conditions for *p*-xylene oxidation, found out in academic studies and widely used in industry (AMOCO process) are as follows: temperature of 180–225 °C, oxygen pressure of 15–30 atm, *p*-xylene to acetic acid molar ratio of 0.08–0.16, and molar ratios Mn/Co and Co:Br being 1:8–10 and 3–4 respectively [2,7,8,48–50]. We have used a temperature of 200 °C, oxygen pressure of 20 atm and molar ratios *p*-xylene/acetic acid and Mn/Co of 0.08 and 1:10 respectively, both in homogeneous and heterogeneous processes. Herein the reaction turnover frequency (TOF) was calculated as the amount of substrate reacted ( $v_{\text{substr}}$ ) per mole of metal ( $v_{(\text{Mn} + \text{Co})}$ ) per unit of time with account of each product yield and the number of oxygen atoms added, according to formula:

$$\text{TOF}(\text{O}_2) = \frac{v_{\text{substr}} * (\omega_{pTAlD} * 1 + \omega_{pTAc} * 2 + \omega_{4-CBA} * 3 + \omega_{TPA} * 4 + \omega_{N/I} * 3)}{v_{(\text{Mn} + \text{Co})} * t},$$

where  $\omega$  is the yield of the certain product, expressed in the unit fractions, N/I is a not identified product (presumably 4-hydroxymethylbenzoic acid) and  $t$  is the minimal reaction time, for which the reaction progress is measured. The results obtained are listed in Table 2.

**Table 2.** Comparison of homogeneous system  $\text{Mn}(\text{OAc})_2/\text{Co}(\text{OAc})_2$  and heterogeneous  $\text{Mn}^{\text{II}}_1\text{Co}^{\text{II}}_{10}@MCM-41/\text{HNT}$  catalyst in the liquid-phase oxidation of *p*-xylene<sup>1</sup>.

Entry	Catalyst	Conv., %	Product Yields, % mol.					TOF, h <sup>-1</sup>
			pTald	pTac	4-HMBA	4-CBA	TPA	
1	$\text{Mn}(\text{OAc})_2/\text{Co}(\text{OAc})_2$	98.0	0.15	0.95	1.2	0.5	95.2	37.5
2	$\text{Mn}^{\text{II}}_1\text{Co}^{\text{II}}_{10}@MCM-41/\text{HNT}$	99.0	0.2	1.0	4.0	-	93.8	142.5

<sup>1</sup> Reaction conditions are: 0.5 mL (4.055 mmol) of *p*-xylene, 5 mL of AcOH, 4.5 mg (0.038 mmol) of KBr, 200 °C, 20 atm of O<sub>2</sub>, 3 h—for both homogeneous and heterogeneous processes; 32 mg (0.127 mmol) of  $\text{Co}(\text{OAc})_2$  and 3.1 mg (0.13 mmol) of  $\text{Mn}(\text{OAc})_2$  for homogeneous system; 150 mg of bimetallic catalyst for the heterogeneous system.

As one can see, both the homogeneous  $\text{Mn}(\text{OAc})_2/\text{Co}(\text{OAc})_2$  system and heterogeneous  $\text{Mn}^{\text{II}}_1\text{Co}^{\text{II}}_{10}@MCM-41/\text{HNT}$  catalyst give a quantitative conversion and similar product distribution with a TPA yield of 94–95% within 3 h (Table 2). Similar results were obtained earlier for  $\mu$ -oxo-bridged complexes of Mn and Co, encapsulated into the zeolite Y pores [16]. It should be noted, that near to the quantitative yield of terephthalic acid in the presence of heterogeneous hierarchical catalyst  $\text{Mn}^{\text{II}}_1\text{Co}^{\text{II}}_{10}@MCM-41/\text{HNT}$  was achieved at much higher substrate to the Mn + Co ratio, giving rise to the higher TOF value (Table 2). It proves the efficacy of the new heterogeneous catalyst developed, comprising of the MCM-41/HNT composite, for the AMOCO process. On the other hand, due to the same loading of KBr for both homogeneous and heterogeneous systems, Co:Br in the latter appeared as high as 1:1, resulting in the increased concentration of Br· radicals and, as a consequence, the easier activation of methyl groups in *p*-xylene and *p*-toluic acid molecules.

Temperature, oxygen, pressure and the presence of KBr were found to be crucial factors for the effective *p*-xylene oxidation process, which was in accordance with the literature data [29]. As seen from Table 3, decrease in oxygen pressure down to 5 atm resulted in corresponding decrease in conversion to 88–89%, and *p*-toluic acid appeared as the major reaction product with the yield of 50–63% for both homogeneous and heterogeneous catalysts. Moreover, lower metal loading in heterogeneous system gave rise to a lower rate of further oxidation of *p*-toluic acid, characterized by the higher activation energy [8], resulting in the extremely low yield of terephthalic acid, about 0.5% (Table 3, Entry 2).

**Table 3.** The influence of the oxygen pressure and KBr presence on the effectiveness of the *p*-xylene oxidation<sup>1</sup>.

Entry	Catalyst	<i>P</i> (O <sub>2</sub> ), atm	KBr	Conv., %	Product Yields, % mol.					TOF, h <sup>-1</sup>	
					pTald	pTac	TPAl <sup>d</sup> 2	4-HMBA	4-CBA		TPA
1	$\text{Mn}(\text{OAc})_2/\text{Co}(\text{OAc})_2$	5	Yes	89.1	11.7	49.8	x	12.6	11.8	3.2	19.0
2	$\text{Mn}^{\text{II}}_1\text{Co}^{\text{II}}_{10}@MCM-41/\text{HNT}$	5	Yes	87.9	14.1	62.8	0.25	6.2	4.1	0.4	63.2
3	$\text{Mn}^{\text{II}}_1\text{Co}^{\text{II}}_{10}@MCM-41/\text{HNT}$	20	No	2.2	1.1	0.4	-	0.1	0.1	0.5	1.6

<sup>1</sup> Reaction conditions are: 0.5 mL (4.055 mmol) of *p*-xylene, 5 mL of AcOH, 4.5 mg (0.038 mmol) of KBr, 200 °C, 3 h—for both homogeneous and heterogeneous processes; 150 mg of bimetallic catalyst for heterogeneous system; 32 mg (0.127 mmol) of  $\text{Co}(\text{OAc})_2$  and 3.1 mg (0.13 mmol) of  $\text{Mn}(\text{OAc})_2$  for homogeneous system. <sup>2</sup> TPAl<sup>d</sup> is terephthalic aldehyde.

The removal of KBr from the reaction medium led to abrupt downfall in conversion for heterogeneous  $\text{Mn}^{\text{II}}_1\text{Co}^{\text{II}}_{10}@MCM-41/\text{HNT}$  catalyst even at high oxygen pressure, when all other conditions are equal (Table 3, Entry 3). *p*-Toluic aldehyde was found to be the major reaction product with the yield of 1% only. The results obtained seemed to be connected not only with the absence of the source of Br· radicals, initiating the oxidation stepwise process, but also with the extremely low concentration of Mn<sup>3+</sup> ions in the system, being also responsible for methyl group activation in the substrate. For the successful oxidation of *p*-xylene, Pd-containing systems were suggested [51–53] or compounds, such as *N*-hydroxyphthalimide, being able to generate stable free radicals [8,54,55]. In these cases, however, a very long time (12–48 h) is needed to obtain the yield of terephthalic acid, exceeding 70%.

The influence of temperature on the rate of the *p*-xylene oxidation and product distribution in the presence of Mn<sup>II</sup><sub>1</sub>Co<sup>II</sup><sub>10</sub>@MCM-41/HNT heterogeneous catalyst is presented in Table 4. As one can see, the quantitative yield of terephthalic acid may be obtained in 5 h at 200 °C and in 3 h at 250 °C, and the TOF values being 401.7 and 424.8 h<sup>-1</sup> respectively (Table 4, Entries 6 and 8–9). Hence, an increase in temperature from 200 to 250 °C results in a slight rise of the catalyst activity and, therefore, the oxidation rate only.

**Table 4.** The influence of the temperature on the effectiveness of the *p*-xylene oxidation in the presence of Mn<sup>II</sup><sub>1</sub>Co<sup>II</sup><sub>10</sub>@MCM-41/HNT catalyst <sup>1</sup>.

Entry.	T, °C	t, h	Conv., %	Product Yields, % mol.					TOF, h <sup>-1</sup>
				pTald	pTac	4-HMBA	4-CBA	TPA	
1	150	5	36.8	28.8	5.2	1.9	0.1	0.8	15.7
2	150	3	25.9	21.1	2.5	1.8	-	0.5	
3	150	1	10.2	8.0	0.5	1.5	-	0.2	
4	200	5	99.8	0.1	0.2	2.3	-	97.2	401.7
5	200	3	99.0	0.2	1.0	4.0	-	93.8	
6	200	1	98.8	1.9	11.7	0.2	-	85.0	
7	250	5	100	-	-	0.5	-	99.5	424.8
8	250	3	99.9	-	0.5	1.8	-	97.6	
9	250	1	99.5	-	4.5	2.1	-	92.9	

<sup>1</sup> Reaction conditions are: 150 mg of bimetallic MnCo heterogeneous MCM-41/HNT-based catalyst, 0.5 mL (4.055 mmol) of *p*-xylene, 5 mL of AcOH, 4.5 mg (0.038 mmol) of KBr and 20 atm. of O<sub>2</sub>.

Vice versa, decrease in temperature down to 150 °C led to an abrupt downfall in activity, in accordance with literature data [29,50]. Herein the *p*-xylene conversion did not exceed 40% even after 5 h, with *p*-toluic aldehyde being obtained as the major reaction product (Table 4, Entry 3).

As seen from Tables 2–4, the yield of 4-carboxybenzaldehyde in the presence of heterogeneous Mn<sup>II</sup><sub>1</sub>Co<sup>II</sup><sub>10</sub>@MCM-41/HNT catalyst (under 20 atm of O<sub>2</sub>) did not exceed 0.5%, and 4-hydroxymethylbenzoic acid being formed as the main by-product with the yield up to 5%. At low oxygen pressures the yield of 4-carboxybenzaldehyde increased and reached 12% for homogeneous Mn(OAc)<sub>2</sub>/Co(OAc)<sub>2</sub> system and 4% for heterogeneous Mn<sup>II</sup><sub>1</sub>Co<sup>II</sup><sub>10</sub>@MCM-41/HNT catalyst (Table 3, Entries 1–2). It should be noted, that 4-carboxybenzaldehyde is the undesirable product of *p*-xylene oxidation: it is slowly oxidized to terephthalic acid and cocrystallizes with it at separation due to structural similarity [2,7,8].

One may assume, that, when Mn<sup>II</sup><sub>1</sub>Co<sup>II</sup><sub>10</sub>@MCM-41/HNT is used as the catalyst, the oxidation passed through the intermediate alcohol formation (Scheme 3, right). Due to the low metal content and/or specific microenvironment of active sites in the Mn<sup>II</sup><sub>1</sub>Co<sup>II</sup><sub>10</sub>@MCM-41/HNT catalyst, caused by the interaction of Mn (II) and Co (II) with halloysite and/or MCM-41 matrix, ArCH<sub>2</sub>OO· radical apparently interacted not with Co<sup>2+</sup>, resulting in aldehyde formation, but with each possible reactant molecule, resulting in the alcohol formation. Noticeably, the oxidation of *p*-xylene to *p*-toluic acid mainly proceeded through the formation of *p*-toluic aldehyde, and only traces of *p*-toluic alcohol were observed at low conversions of *p*-xylene. Hence, the “alcohol pathway” was presumably the characteristic of the oxidation *p*-toluic acid. Thus obtained 4-hydroxymethylbenzoic acid underwent further Co (II) catalyzed oxidation to terephthalic acid, initiated by O<sub>2</sub> or Br· as radicals.

We think the explanation above is consistent with the influence of oxygen pressure and KBr observed, as well as with a high reaction rate even at very low metal loading, for the selective oxidation of *p*-xylene to terephthalic acid in the presence of heterogeneous Mn<sup>II</sup><sub>1</sub>Co<sup>II</sup><sub>10</sub>@MCM-41/HNT catalyst. Therefore, MCM-41/HNT composite, doped with Mn and Co, may be considered as a prospective catalyst for the AMOCO process, far superior to the original homogeneous Mn(OAc)<sub>2</sub>/Co(OAc)<sub>2</sub> system.



Unfortunately, metal leaching took place during the reaction. The quantity of leached metals depended on the reaction temperature and time: a higher temperature and longer reaction time resulted in less metal maintained in the catalyst (Table 5). Herein Co leached the first followed by Mn. When carrying out the reaction for the longest time (5 h), the concentrations of both Mn and Co dropped approximately by 13–15 times (Table 5, Entry 5). XPS analysis revealed no Mn or Co on the surface of the samples recycled.

**Table 5.** Comparative Mn and Co weight content in the recycled samples of  $\text{Mn}^{\text{II}}_1\text{Co}^{\text{II}}_{10}$ @MCM-41/HNT catalyst depending on reaction conditions.

Entry	Mn (wt. %)	Co (wt. %)	Reaction Conditions
1	0.15	1.29	Initial catalyst
2	0.15	0.22	150 °C, 20 atm. of O <sub>2</sub> , 3 h
3	0.03	0.13	200 °C, 20 atm. of O <sub>2</sub> , 3 h
4	0.04	0.09	250 °C, 20 atm. of O <sub>2</sub> , 3 h
5	0.01	0.10	200 °C, 20 atm. of O <sub>2</sub> , 5 h

We suppose, the metal leaching observed occurs due to dissolution of the adsorbed Mn and Co species by acetic and hydrobromic acids. The last one is resulted from the interaction of Br· radicals with substrate or intermediate compounds, bearing H-atoms at side carbons (Scheme 3). Nonetheless it should also be noted, that catalyst, based on MCM-41/HNT composite possesses very low packed density and, simultaneously, high apparent adsorption capacity, and, therefore, occupy all of the reaction volume (5 mL of AcOH vs. 150 mg of catalyst). To extract reaction products for HPLC analysis, up to 40 mL of DMSO (the best solvent for terephthalic and *p*-toluic acids) was required, that strictly reduced the possibility for the hot filtration and recycling tests. Mn and Co content in the catalyst recycled was measured just after filtration from DMSO solution. Therefore, the metal leaching could take place not only during the reaction, but also at washing by DMSO.

Hence one may conclude, that pores and cavities of MCM-41 and halloysite moieties act as microreactors for the oxidation of *p*-xylene under the reaction conditions. However these pores appear too wide and not able to effectively retain Mn and Co species inside the carrier at filtration and washing as compared with polynuclear  $\mu_3$ -oxo-bound complexes of Co and Mn, encapsulated in the cavities of Y zeolite [16]. This challenges for the further development and modification of MCM-41/HNT composites to provide more effective metal retention and leaching resistance under the severe reaction conditions, to make possible the repeated use of  $\text{Mn}^{\text{II}}_1\text{Co}^{\text{II}}_{10}$ @MCM-41/HNT catalyst in *p*-xylene oxidation.

### 3. Experimental

#### 3.1. Chemicals

The following substances were used as substrates and reference compounds: *p*-xylene 4-H<sub>3</sub>CC<sub>6</sub>H<sub>4</sub>CH<sub>3</sub> (pX; Reachim, Purum, Moscow, Russia); *p*-toluic aldehyde 4-H<sub>3</sub>CC<sub>6</sub>H<sub>4</sub>C(=O)H (pTAlD) (Aldrich, 97%; Steinheim, Germany); *p*-toluic acid 4-H<sub>3</sub>CC<sub>6</sub>H<sub>4</sub>C(=O)OH (pTAc; Aldrich, 98%; Steinheim, Germany); 4-carboxybenzaldehyde 4-HO(O=)CC<sub>6</sub>H<sub>4</sub>C(=O)H (4-CBA; Aldrich, 97%; Steinheim, Germany) and terephthalic acid *p*-HO(O=)CC<sub>6</sub>H<sub>4</sub>C(=O)OH (TPA; Acros Organics, 99+%; Geel, Belgium).

For the synthesis of Mn/Co oxidation catalyst based on MCM-41/HNT composite the following reagents were used: manganese (II) acetate tetrahydrate (CH<sub>3</sub>COO)<sub>2</sub>Mn × 4H<sub>2</sub>O (Aldrich, ≥99%; Steinheim, Germany), cobaltous (II) acetate tetrahydrate CH<sub>3</sub>COO)<sub>2</sub>Co × 4H<sub>2</sub>O (Aldrich, ≥98%; Steinheim, Germany) and MCM-41/HNT composite, earlier prepared according to literature procedure [24].

Acetic acid  $\text{CH}_3\text{COOH}$  (Chimmed, Chemical Grade; Moscow, Russia), dimethyl sulfoxide (DMSO)  $(\text{H}_3\text{C})_2\text{SO}$  (Ruschim, Imp; Moscow, Russia) and potassium bromide  $\text{KBr}$  (Chimmed, Chemical Grade; Moscow, Russia) were used as solvent and additive respectively in the procedure of catalytic experiments.

Double-distilled water, methanol  $\text{CH}_3\text{OH}$  (J.T. Baker, HPLC grade; Gliwice, Poland) and acetonitrile  $\text{CH}_3\text{CN}$  (J.T. Baker, HPLC grade; Gliwice, Poland) were used as solvents and phosphoric acid  $\text{H}_3\text{PO}_4$  (Component-Reactive, Chemical Grade; Moscow, Russia) was used as a pH regulating additive while conducting HPLC analysis.

### 3.2. Analyses and Instrumentations

Analysis by transmission electron microscopy (TEM) was carried out using LEO912 AB OMEGA (Carl Zeiss, Jena, Germany) and JEM-2100 JEOL microscopes (Jeol Ltd., Tokyo, Japan) with an electron tube voltage of 100 kV.

The isotherms of nitrogen adsorption/desorption were measured at 77 K on Micromeritics Gemini VII 2390 t instrument (Micromeritics Instrument Corp., Norcross, GA, USA). Before the measurements, the samples were degassed at 350 °C for 4 h. The specific surface area was calculated with the Brunauer–Emmett–Teller (BET) and Langmuir methods applied to the range of relative pressures  $P/P_0 = 0.05\text{--}0.30$ . The pore volume and pore size distributions were determined from the adsorption branches of the isotherms based on the Barrett–Joyner–Halenda (BJH) model.

Weight content of manganese and cobalt in the catalyst was determined by means of atomic emission spectroscopy with inductively coupled plasma (ICP-AES) and X-ray fluorescent spectrometry (XFS). ICP-AES analysis was performed on the IRIS Intrepid II XPL instrument (Thermo Electron Corp., Waltham, MA, USA) in the radial observation modes at wavelengths of 257.6 and 259.4 nm for Mn and 228.6 and 237.9 nm for Co. XFS analysis was conducted on the ARL PERFORM'X spectrometer (Thermo Fisher Scientific, Waltham, MA, USA) with Rh anode and tube diameter of 3 mm in the etalon-free mode with the relative error of 5%.

X-ray photoelectron studies (XPS) were carried out on a Versa Probe II instrument (ULVAC-PHI Inc., Hagisono, Chigasaki, Kanagawa, Japan), equipped with a photo-electronic hemispherical analyzer with retarding potential OPX-150. X-ray radiation of the aluminum anode ( $\text{Al K}\alpha = 1486.6$  eV) with a tube voltage of 12 kV, emission current of 20 mA and power of 50 W was used to excite photoelectrons. Photoelectron peaks were calibrated with respect to the carbon C 1s line with a binding energy of 284.8 eV.

Qualitative and quantitative analysis for the products of the *p*-xylene oxidation was carried out by means of high-performance liquid chromatography (HPLC) similar to the procedure, earlier described in literature [56] on the Agilent 1100 Series instrument (Agilent Technologies, Santa Clara, CA, USA) with a Zorbax SB-C<sub>18</sub> column (5  $\mu\text{m}$ , 2.1 mm  $\times$  150 mm) and UV detector. The eluent consisted of methanol (25%), acetonitrile (25%) and water (50%). For better peak resolution, phosphoric acid was added with concentration of 1 mL per 1 L of the eluent. The flow rate was 0.1 mL/min and the injection volume was 0.1  $\mu\text{L}$ . Chromatograms were recorded at 210, 230, 254 and 280 nm simultaneously and analyzed on a computer using Agilent 1100 Software (Agilent Technologies, 2008, Santa Clara, CA, USA). Conversion of *p*-xylene and the yield of each oxidation product were calculated using calibrating curves with exponential approximation.

### 3.3. The Synthesis of Mn/Co-Containing Oxidation Catalyst Based on the MCM-41/HNT Composite

Deposition of Mn and Co on the MCM-41/HNT composite was performed according to the following procedure [16]. Of MCM-41/HNT composite 1000 mg and 20 mL of distilled water were placed into a 100 mL one-neck round-bottom flask, equipped with a reflux condenser and a magnetic stirrer. Then 20 mg of  $\text{Mn}(\text{OAc})_2 \times 4\text{H}_2\text{O}$  (0.08 mmol) and 200 mg of  $\text{Co}(\text{OAc})_2 \times 4\text{H}_2\text{O}$  (0.8 mmol) were placed into a chemical beaker and dissolved in 10 mL of distilled water at room temperature while stirring. Then the resulting solution of the pink-purple color was added dropwise to the suspension

of MCM-41/HNT composite in water at room temperature while stirring, and additional 10 mL of distilled water was passed through the dropping funnel to wash the residues of  $\text{Mn}(\text{OAc})_2$  and  $\text{Co}(\text{OAc})_2$  solution. The reaction was carried out at 60 °C for 12 h. After that the material obtained was centrifuged, washed twice with ethanol for the better removal of water and then dried in the air. The catalyst obtained was isolated as a pale-pink powder, weighing 1065 mg (92%).

$\omega_{\text{Mn}}$  (XFS): 0.15%.

$\omega_{\text{Co}}$  (XFS): 1.29%.

XPS (eV): 74.5 ( $\text{Al}_2\text{O}_3$ , Al 2p, 2.5%); 103.5 ( $\text{SiO}_2$ , Si 2p, 25.9%); 119.5 ( $\text{Al}_2\text{O}_3$ , Al 2s); 154.5 ( $\text{SiO}_2$ , Si 2s); 284.9 ( $-\text{CH}_2\text{CH}_2-$ , C 1s, 1.27%), 285.9 ( $-\text{CH}_2\text{CH}_2\text{N}$ ,  $\text{H}_3\text{CC}(\text{=O})-$ , C 1s, 3.15%), ( $\text{H}_3\text{CC}(\text{=O})-$ ,  $-\text{CH}_2\text{N}^+$ , C 1s, 0.82%), 290.1 ( $\text{H}_3\text{CC}(\text{=O})-$ , C 1s sat, 0.55%); 400.5 ( $-\text{CH}_2\text{CH}_2\text{N}$ ,  $[\text{NR}_4]^+$ , N 1s, 0.6%); 530.6 ( $\text{MnO}_x$ ,  $\text{CoO}_x$ , O 1s, 1.7%), 532.1 ( $\text{CH}_3\text{C}(\text{=O})\text{O}-$ , ( $\text{Al}_2\text{O}_3$ ) $_x$ ( $\text{SiO}_2$ ) $_y$ , O 1s, 14.8%), 533.1 ( $\text{SiO}_2$ , O 1s, 43.0%), 534.6 (O ...  $\text{H}_2\text{O}$ , O 1s, 4.6%); 642.5 ( $\text{MnO}$ , Mn 2p $_{3/2}$ , 0.08%), 646.9 ( $[\text{MnO}_4]$  bound, Mn 2p $_{3/2}$ , 0.02%), 654.0 ( $\text{MnO}$ , Mn 2p $_{1/2}$ ), ( $[\text{MnO}_4]$  bound, Mn 2p $_{1/2}$ ); 686.5 (O-Si-F, F 1s, 0.2%); 780.0 ( $\text{CoO}$ , Co 2p $_{3/2}$ , 0.05%), 782.5 ( $[\text{CoO}_6]$  bound, Co 2p $_{3/2}$ , 0.28%), 785.2 ( $\text{CoO}$ ,  $[\text{CoO}_6]$  bound, Co 2p $_{3/2}$  sat, 0.14%), 788.2 ( $\text{CoO}$ ,  $[\text{CoO}_6]$  bound, Co 2p $_{3/2}$  sat, 0.17%), 791.6 (Co 2p $_{3/2}$  sat, 0.06%), 794.6 ( $\text{CoO}$ , Co 2p $_{1/2}$ ), 798.4 ( $[\text{CoO}_6]$  bound, Co 2p $_{1/2}$ ), 802.4 ( $\text{CoO}$ ,  $[\text{CoO}_6]$  bound, Co 2p $_{1/2}$  sat), 805.1 ( $\text{CoO}$ ,  $[\text{CoO}_6]$  bound, Co 2p $_{1/2}$  sat), 808.9 (Co 2p $_{1/2}$  sat, 0.06%).

### 3.4. Protocol for the Catalytic Experiments

Oxidation of *p*-xylene in the presence of Mn/Co MCM-41/HNT catalyst was carried out according to the literature procedures [16,29]. Here 150 mg of the catalyst, 4.5 mg of KBr, 0.5 mL of *p*-xylene and 5 mL of acetic acid were placed in a titanium autoclave, equipped with a magnetic stirrer. The autoclave was sealed, filled with oxygen up to a pressure of 2 MPa and placed in an oven with a thermostat control. Then the oxidation reaction was conducted at 150, 200 or 250 °C for 1, 3 or 5 h. After reaction, the autoclave was cooled down to room temperature and depressurized. The reaction products were additionally diluted by DMSO as the best solvent for terephthalic acid and, after the catalyst sedimentation and filtration, analyzed by the HPLC method.

The catalyst activity (TOF = turnover frequency) was calculated as the amount of reacted substrate ( $v_{\text{substr}}$ ) per mole of metal ( $v_{(\text{Mn} + \text{Co})}$ ) per unit of time with account of the yield of each product and number the oxygen atoms added, according to the formula:

$$\text{TOF}(\text{O}_2) = \frac{v_{\text{substr}} * (\omega_{p\text{TAla}}*1 + \omega_{p\text{TAc}}*2 + \omega_{4\text{-CBA}}*3 + \omega_{\text{TPA}}*4 + \omega_{\text{N/I}}*3)}{v_{(\text{Mn}+\text{Co})} * t},$$

where  $\omega$  is the yield of the certain product, expressed in the unit fractions, N/I is a not identified product (presumably 4-hydroxymethylbenzoic acid) and  $t$  is the minimal reaction time, for which the reaction progress is measured.

Each experiment at the same conditions was carried out two or three times, with the results differing by no more than 5% from the corresponding average value. These average values were presented in Tables 2–4. The measurement error did not exceed 5%.

## 4. Conclusions

Heterogeneous bimetallic Mn/Co-containing catalyst, based on MCM-41/halloysite composite, have been synthesized for the first time and tested in *p*-xylene oxidation under the conditions of the AMOCO process. It was demonstrated, that in the presence of bimetallic heterogeneous catalyst  $\text{Mn}^{\text{II}}_1\text{Co}^{\text{II}}_{10}\text{@MCM-41/HNT}$  and KBr as a free radical source, the quantitative yield of terephthalic acid can be obtained in 3 h at temperature of above 200 °C, and oxygen pressure of 20 atm. The substrate to the Mn + Co ratio was 3.5–4 times higher than that for the traditional homogeneous

Mn(OAc)<sub>2</sub>/Co(OAc)<sub>2</sub> system, hence proving a high efficacy and superiority of the heterogeneous catalyst, based on the hierarchical material MCM-41/HNT.

The influence of the oxygen pressure, temperature and KBr presence on the catalyst activity and product distribution was investigated. It was established that a decrease in oxygen pressure to 5 atm. resulted in the corresponding decrease of *p*-xylene conversion to 88–89%, with *p*-toluic acid obtained as the major reaction product with the yield up to 63% within 3 h. Decrease in temperature from 200 to 150 °C led to the abrupt downfall in the reaction rate. Herein the conversion did not exceed 40% after 5 h and *p*-toluic aldehyde was the major reaction product. Vice versa, rise in temperature from 200 to 250 °C did not result in the significant increase of the reaction turnover frequency. The presence of KBr was found to be crucial for the effective process of the oxidation of *p*-xylene, whose conversion did not exceed 2%, when KBr was removed from the reaction medium.

It was found that in the presence of Mn<sup>II</sup><sub>1</sub>Co<sup>II</sup><sub>10</sub>@MCM-41/HNT the further oxidation of *p*-toluic acid to terephthalic acid mostly proceeded through the formation of 4-hydroxymethylbenzoic acid, thus eliminating the stage of undesirable 4-carboxybenzaldehyde. This pathway supposes the diminished role of the Co (II) in the oxidation of *p*-toluic acid and, therefore, allows the elevated substrate to catalyst ratios, but requires high oxygen pressures and Br· radicals as initiators.

Halloysite clay is a cheap and available in thousands tons aluminosilicate, which makes it a prospective nanomaterial for catalysts support. Despite the low resistant to metal leaching under the reaction and separation conditions the heterogeneous catalyst showed a phenomenally high activity in the oxidation of *p*-xylene to terephthalic acid under the conditions of AMOCO industrial process. This Mn<sup>II</sup><sub>1</sub>Co<sup>II</sup><sub>10</sub>@MCM-41/HNT catalyst based on new hierarchical support with halloysite aluminosilicate nanotubes could be easily scaled up after stability improvement.

**Author Contributions:** Conceptualization, A.G., V.V. and A.M.; Methodology, A.G. and A.Z.; Software, A.Z. and E.I.; Validation, E.K. and A.M.; Formal analysis, E.I.; Investigation, A.Z. and A.G.; Resources, E.I.; Data curation, A.Z.; Writing—Original draft preparation, A.Z. and A.G.; Writing—Review and editing, A.M. and E.K.; Visualization, A.G. and A.Z.; Supervision, V.V.; Project administration, V.V. and A.M.; Funding acquisition, E.I. All authors have read and agreed to the published version of the manuscript.

**Funding:** The study was financially supported by the Ministry of Science and Higher Education of the Russian Federation, the unique project identifier is RFMEFI57717X0239.

**Acknowledgments:** We also thank National University of Science and Technology ‘MISIS’ (Moscow, Russia) for XPS facilities and Valentine Stytsenko (Gubkin University) and Yusuf Darrat (Louisiana Tech University, USA) for language editing.

**Conflicts of Interest:** The authors declare no conflict of interest.

## References

1. Sheehan, R.J. Terephthalic acid, dimethyl terephthalate, and isophthalic acid. In *Ullmann's Encyclopedia of Industrial Chemistry*; Wiley-VCH Verlag GmbH & Co. KGaA: Weinheim, Germany, 2002.
2. Nazimok, V.F.; Ovchinnikov, V.I.; Potekhin, V.M. *Liquid-Phase Oxidation of Alkyl Aromatic Hydrocarbons*; Chemistry: Moscow, Russia, 1987; p. 240. (In Russian)
3. Li, M.; Niu, F.; Zuo, X.; Metelski, P.D.; Busch, D.H.; Subramaniam, B. A spray reactor concept for catalytic oxidation of *p*-xylene to produce high-purity terephthalic acid. *Chem. Eng. Sci.* **2013**, *104*, 93–102. [[CrossRef](#)]
4. Partenheimer, W. Methodology and scope of metal/bromide autoxidation of hydrocarbons. *Catal. Today* **1995**, *23*, 69–158. [[CrossRef](#)]
5. Saffer, A.; Barker, R.S. Preparation of Aromatic Polycarboxylic Acids. U.S. Patent 2833816 A, 6 May 1958.
6. Saffer, A.; Barker, R.S. Oxidation Chemical Process. U.S. Patent 3089906 A, 14 May 1963.
7. Karakhanov, E.A.; Maksimov, A.L.; Zolotukhina, A.V.; Vinokurov, V.A. Oxidation of *p*-xylene. A review. *Russ. J. Appl. Chem.* **2018**, *91*, 707–727. [[CrossRef](#)]
8. Tomás, R.A.F.; Bordado, J.C.M.; Gomes, J.F.P. *p*-xylene oxidation to terephthalic acid: A literature review oriented toward process optimization and development. *Chem. Rev.* **2013**, *113*, 7421–7469. [[CrossRef](#)] [[PubMed](#)]

9. Ichikawa, Y.; Yamashita, G.; Tokashiki, M.; Yamaji, T. New Oxidation Process for Production of Terephthalic Acid from *p*-Xylene. *Ind. Eng. Chem.* **1970**, *62*, 38–42. [[CrossRef](#)]
10. Fadzil, N.A.M.; Rahim, M.H.A.; Maniam, G.P. A brief review of *para*-xylene oxidation to terephthalic acid as a model of primary C–H bond activation. *Chin. J. Catal.* **2014**, *35*, 1641–1652. [[CrossRef](#)]
11. Zuo, X.; Subramaniam, B.; Busch, D.H. Liquid-phase oxidation of toluene and *p*-toluic acid under mild conditions: Synergistic effects of cobalt, zirconium, ketones, and carbon dioxide. *Ind. Eng. Chem. Res.* **2008**, *47*, 546–552. [[CrossRef](#)]
12. Sun, W.; Yi, P.; Zhao, L.; Zhou, X. Simplified free-radical reaction kinetics for *p*-xylene oxidation to terephthalic acid. *Chem. Eng. Technol.* **2008**, *31*, 1402–1409. [[CrossRef](#)]
13. Zuo, X.; Niu, F.; Snavely, K.; Subramaniam, B.; Busch, D.H. Liquid phase oxidation of *p*-xylene to terephthalic acid at medium-high temperatures: Multiple benefits of CO<sub>2</sub>-expanded liquids. *Green Chem.* **2010**, *12*, 260–267. [[CrossRef](#)]
14. Hronec, M.; Hrabě, Z. Liquid-phase oxidation of *p*-xylene catalyzed by metal oxides. *Ind. Eng. Chem. Prod. Res. Develop.* **1986**, *25*, 257–261. [[CrossRef](#)]
15. Li, Y.; Duan, D.; Wu, M.; Li, J.; Yan, Z.; Wang, W.; Zi, G.; Wang, J. One-step synthesis of 2,5-dihydroxyterephthalic acid by the oxidation of *p*-xylene over M-MCM-41 (M = Fe, Fe/Cu, Cu) catalysts. *Chem. Eng. J.* **2016**, *306*, 777–783. [[CrossRef](#)]
16. Chavan, S.A.; Srinivas, D.; Ratnasamy, P. Selective oxidation of *para*-xylene to terephthalic acid by  $\mu_3$ -oxo-bridged Co/Mn cluster complexes encapsulated in zeolite-Y. *J. Catal.* **2001**, *204*, 409–419. [[CrossRef](#)]
17. Lvov, Y.; Wang, W.; Zhang, L.; Fakhrullin, R. Halloysite clay nanotubes for loading and sustained release of functional compounds. *Adv. Mater.* **2016**, *28*, 1227–1250. [[CrossRef](#)] [[PubMed](#)]
18. Vinokurov, V.A.; Stavitskaya, A.V.; Chudakov, Y.A.; Ivanov, E.V.; Shrestha, L.K.; Ariga, K.; Darrat, Y.A.; Lvov, Y.M. Formation of metal clusters in halloysite clay nanotubes. *Sci. Technol. Adv. Mater.* **2017**, *18*, 147–151. [[CrossRef](#)]
19. Vinokurov, V.A.; Stavitskaya, A.V.; Glotov, A.P.; Novikov, A.A.; Zolotukhina, A.V.; Kotelev, M.S.; Gushchin, P.A.; Ivanov, E.V.; Darrat, Y.; Lvov, Y.M. Nanoparticles formed onto/into halloysite clay tubules: Architectural synthesis and applications. *Chem. Rec.* **2018**, *18*, 858–867. [[CrossRef](#)]
20. Vinokurov, V.; Glotov, A.; Chudakov, Y.; Stavitskaya, A.; Ivanov, E.; Gushchin, P.; Zolotukhina, A.; Maximov, A.; Karakhanov, E.; Lvov, Y. Core/shell ruthenium–halloysite nanocatalysts for hydrogenation of phenol. *Ind. Eng. Chem. Res.* **2017**, *56*, 14043–14052. [[CrossRef](#)]
21. Glotov, A.; Stavitskaya, A.; Chudakov, Y.; Ivanov, E.; Huang, W.; Vinokurov, V.; Zolotukhina, A.; Maximov, A.; Karakhanov, E.; Lvov, Y. Mesoporous metal catalysts templated on clay nanotubes. *Bull. Chem. Soc. Jpn.* **2019**, *92*, 61–69. [[CrossRef](#)]
22. Glotov, A.; Stytsenko, V.; Artemova, M.; Kotelev, M.; Ivanov, E.; Gushchin, P.; Vinokurov, V. Hydroconversion of aromatic hydrocarbons over bimetallic catalysts. *Catalysts* **2019**, *9*, 38. [[CrossRef](#)]
23. Glotov, A.P.; Stavitskaya, A.V.; Chudakov, Y.A.; Artemova, M.I.; Smirnova, E.M.; Demikhova, N.R.; Shabalina, T.N.; Gureev, A.A.; Vinokurov, V.A. Nanostructured ruthenium catalysts in hydrogenation of aromatic compounds. *Petrol. Chem.* **2018**, *58*, 1221–1226. [[CrossRef](#)]
24. Glotov, A.; Levshakov, N.; Stavitskaya, A.; Artemova, M.; Gushchin, P.; Ivanov, E.; Vinokurov, V.; Lvov, Y. Templated self-assembly of ordered mesoporous silica on clay nanotubes. *Chem. Commun.* **2019**, *55*, 5507–5510. [[CrossRef](#)]
25. Lvov, Y.; Panchal, A.; Fu, Y.; Fakhrullin, R.; Kryuchkova, M.; Batasheva, S.; Stavitskaya, A.; Glotov, A.; Vinokurov, V. Interfacial self-assembly in halloysite nanotube composites. *Langmuir* **2019**, *35*, 8646–8865. [[CrossRef](#)] [[PubMed](#)]
26. Glotov, A.; Levshakov, N.; Vutolkina, A.; Lysenko, S.; Karakhanov, E.; Vinokurov, V. Aluminosilicates supported La-containing sulfur reduction additives for FCC catalyst: Correlation between activity, support structure and acidity. *Catal. Today* **2019**, *329*, 135–141. [[CrossRef](#)]
27. Glotov, A.P.; Levshakov, N.S.; Vutolkina, A.V.; Lysenko, S.V.; Gushchin, P.A.; Vinokurov, V.A. Bimetallic sulfur reduction additives based on aluminosilicate of Al-MCM-41 type for cracking catalysts: Desulfurizing activity vs. ratio of components in a support. *Russ. J. Appl. Chem.* **2019**, *92*, 562–568. [[CrossRef](#)]
28. Karakhanov, E.; Akopyan, A.; Golubev, O.; Anisimov, A.; Glotov, A.; Vutolkina, A.; Maximov, A. Alkali earth catalysts based on mesoporous MCM-41 and Al-SBA-15 for sulfone removal from middle distillates. *ACS Omega* **2019**, *4*, 12736–12744. [[CrossRef](#)] [[PubMed](#)]



29. Ghiaci, M.; Mostajeran, M.; Gil, A. Synthesis and characterization of Co–Mn nanoparticles immobilized on a modified bentonite and its application for oxidation of *p*-xylene to terephthalic acid. *Ind. Eng. Chem. Res.* **2012**, *51*, 15821–15831. [[CrossRef](#)]
30. Carver, J.C.; Schweitzer, G.K.; Carlson, T.A. Use of X-Ray Photoelectron Spectroscopy to Study Bonding in Cr, Mn, Fe, and Co Compounds. *J. Chem. Phys.* **1972**, *57*, 973–981. [[CrossRef](#)]
31. Franzen, H.F.; Umana, M.X.; McCreary, J.R.; Thorn, R.J. XPS spectra of some transition metal and alkaline earth monochalcogenides. *J. Solid State Chem.* **1976**, *18*, 363–368. [[CrossRef](#)]
32. Tan, B.J.; Klabunde, K.J.; Sherwood, P.M.A. XPS studies of solvated metal atom dispersed (SMAD) catalysts. Evidence for layered cobalt-manganese particles on alumina and silica. *J. Am. Chem. Soc.* **1991**, *113*, 855–861. [[CrossRef](#)]
33. McIntyre, N.S.; Cook, M.G. X-ray photoelectron studies on some oxides and hydroxides of cobalt, nickel, and copper. *Anal. Chem.* **1975**, *47*, 2208–2213. [[CrossRef](#)]
34. Mc Intyre, N.S.; Johnston, D.D.; Coatsworth, L.L.; Davidson, R.D.; Brown, J.R. X-ray photoelectron spectroscopic studies of thin film oxides of cobalt and molybdenum. *Surf. Interface Anal.* **1990**, *15*, 265–272. [[CrossRef](#)]
35. Kim, K.S. X-ray-photoelectron spectroscopic studies of the electronic structure of CoO. *Phys. Rev. B* **1975**, *11*, 2177–2185. [[CrossRef](#)]
36. Umezawa, Y.; Reilley, C.N. Effect of argon ion bombardment on metal complexes and oxides studied by x-ray photoelectron spectroscopy. *Anal. Chem.* **1978**, *50*, 1290–1295. [[CrossRef](#)]
37. Oku, M. X-ray photoelectron spectra of KMnO<sub>4</sub> and K<sub>2</sub>MnO<sub>4</sub> fractured in situ. *J. Electron Spectrosc. Relat. Phenom.* **1995**, *74*, 135–148. [[CrossRef](#)]
38. Brown, D.G.; Weser, U. XPS spectra of spin-triplet cobalt (III) complexes. *Z. Nat. B* **1979**, *34*, 1468–1470. [[CrossRef](#)]
39. Nefedov, V.I.; Baranovskii, I.B.; Molodkin, A.K.; Omuralieva, V.O. X-ray photoelectron study of cobalt compounds. *Russ. J. Inorg. Chem.* **1973**, *18*, 1295. (In Russian)
40. Nefedov, V.I.; Gati, D.; Dzhurinskii, B.F.; Sergushin, N.P.; Salyn, Y.V. X-ray photoelectron study of several elements oxides. *Russ. J. Inorg. Chem.* **1975**, *20*, 2307. (In Russian)
41. Nefedov, V.I.; Firsov, M.N.; Shaplygin, I.S. Electronic structures of MRhO<sub>2</sub>, MRh<sub>2</sub>O<sub>4</sub>, RhMO<sub>4</sub> and Rh<sub>2</sub>MO<sub>6</sub> on the basis of X-ray spectroscopy and ESCA data. *J. Electron Spectrosc. Relat. Phenom.* **1982**, *26*, 65–78. [[CrossRef](#)]
42. Molinaro, F.S.; Little, R.G.; Ibers, J.A. Oxygen binding to a model for the active site in cobalt-substituted hemoglobin. *J. Am. Chem. Soc.* **1977**, *99*, 5628–5632. [[CrossRef](#)]
43. Emara, A.A.A.; Ali, A.M.; El-Asmy, A.F.; Ragab, E.-S.M. Investigation of the oxygen affinity of manganese (II), cobalt (II) and nickel (II) complexes with some tetradentate Schiff bases. *J. Saudi Chem. Soc.* **2011**, *18*, 762–773. [[CrossRef](#)]
44. Beamson, G.; Briggs, D. *High Resolution XPS of Organic Polymers: The Scienta ESCA300 Database*; John Wiley & Sons: Chichester, UK, 1992; 295p.
45. Briggs, D.; Beamson, G. Primary and secondary oxygen-induced C 1s binding energy shifts in X-ray photoelectron spectroscopy of polymers. *Anal. Chem.* **1992**, *64*, 1729–1736. [[CrossRef](#)]
46. Yuan, H.; Fang, X.; Ma, Q.; Mao, J.; Chen, K.; Chen, Z.; Li, H. New mechanistic insight into the aerobic oxidation of methylaromatic compounds catalyzed by Co–Mn–Br and its applications. *J. Catal.* **2016**, *339*, 284–291. [[CrossRef](#)]
47. Wang, Q.; Li, X.; Wang, L.; Cheng, Y.; Xie, G. Effect of water content on the kinetics of *p*-xylene liquid-phase catalytic oxidation to terephthalic acid. *Ind. Eng. Chem. Res.* **2005**, *44*, 4518–4522. [[CrossRef](#)]
48. Li, M.; Niu, F.; Busch, D.H.; Subramaniam, B. Kinetic investigations of *p*-xylene oxidation to terephthalic acid with a Co/Mn/Br catalyst in a homogeneous liquid phase. *Ind. Eng. Chem. Res.* **2014**, *53*, 9017–9026. [[CrossRef](#)]
49. Cheng, Y.; Li, X.; Wang, L.; Wang, Q. Optimum ratio of Co/Mn in the liquid-phase catalytic oxidation of *p*-xylene to terephthalic acid. *Ind. Eng. Chem. Res.* **2006**, *45*, 4156–4162. [[CrossRef](#)]
50. Li, K.; Li, S. CoBr<sub>2</sub>–MnBr<sub>2</sub> containing catalysts for catalytic oxidation of *p*-xylene to terephthalic acid. *Appl. Catal. A Gen.* **2008**, *340*, 271–277. [[CrossRef](#)]

51. Liu, H.; Chen, G.; Jiang, H.; Li, Y.; Luque, R. From alkyl aromatics to aromatic esters: Efficient and selective C–H activation promoted by a bimetallic heterogeneous catalyst. *ChemSusChem* **2012**, *5*, 1892–1896. [[CrossRef](#)] [[PubMed](#)]
52. Kesavan, L.; Tiruvalam, R.; Ab Rahim, M.H.; bin Saiman, M.I.; Enache, D.I.; Jenkins, R.L.; Dimitratos, N.; Lopez-Sanchez, J.A.; Taylor, S.H.; Knight, D.W.; et al. Solvent-free oxidation of primary carbon-hydrogen bonds in toluene using Au-Pd alloy nanoparticles. *Science* **2011**, *331*, 195–199. [[CrossRef](#)] [[PubMed](#)]
53. Tibitt, J.M.; Gong, W.H.; Schammel, W.P.; Hepfer, R.P.; Adamian, V.; Brugge, S.P.; Metelski, P.D.; Zhou, C. Process for the Production of Aromatic Carboxylic Acids in Water. WO Patent 2007133976 A2, 22 November 2007.
54. Tashiro, Y.; Iwahama, T.; Sakaguchi, S.; Ishii, Y. A new strategy for the preparation of terephthalic acid by the aerobic oxidation of *p*-xylene using *N*-hydroxyphthalimide as a catalyst. *Adv. Synth. Catal.* **2001**, *343*, 220–225. [[CrossRef](#)]
55. Saha, B.; Koshino, N.; Espenson, J.H. *N*-hydroxyphthalimides and metal cocatalysts for the autoxidation of *p*-xylene to terephthalic acid. *J. Phys. Chem. A* **2004**, *108*, 425–431. [[CrossRef](#)]
56. Xiao, Y.; Zhang, X.Y.; Wang, Q.B.; Tan, Z.; Guo, C.C.; Deng, W.; Liu, Z.G.; Zhang, H.F. The preparation of terephthalic acid by solvent-free oxidation of *p*-xylene with air over T(*p*-Cl)PPMnCl and Co(OAc)<sub>2</sub>. *Chin. Chem. Lett.* **2011**, *22*, 135–138. [[CrossRef](#)]



© 2019 by the authors. Licensee MDPI, Basel, Switzerland. This article is an open access article distributed under the terms and conditions of the Creative Commons Attribution (CC BY) license (<http://creativecommons.org/licenses/by/4.0/>).